Multiloop Diagrams in Non-Relativistic Field Theories and the Deuteron Quadrupole Moment

Michael Binger
Department of Physics, North Carolina State University
Raleigh, North Carolina 27695-8202 USA

Abstract

A new method is developed to calculate multiloop Feynman diagrams in non-relativistic field theories. A consistent scheme for regularizing and renormalizing loop integrals is established and shown to reproduce the results of dimensional regularization (DR) and modified minimal subtraction ($\overline{MS}$) or DR and power divergence subtraction (PDS) up to next-to-leading order (NLO). However, significantly less effort is required to evaluate the integrals and the methods are easily generalized to higher order graphs. Thus, even the most complicated multiloop graph can be expressed in terms of analytic functions. These techniques are then used to calculate the quadrupole moment of the deuteron to three loops in the Kaplan, Savage, and Wise effective field theory. A new unfixed direct $S \to D$ wave counterterm occurs at this order and its value is determined.

I. INTRODUCTION

Recent progress in effective field theory [1] has made possible the calculation of many properties of nuclear systems in a perturbative expansion [2–6]. The progress is largely based on a consistent power counting developed by Kaplan, Savage, and Wise (KSW) which accounts for the large scattering lengths in the two nucleon sector by utilizing dimensional regularization and a unique subtraction scheme called power divergence subtraction (PDS). However, higher order graphs very quickly become intractable with the standard techniques of dimensional regularization and Feynman parameters. This is because combining three dimensional propagators in the usual way leads to square roots of polynomials of the Feynman parameters and one quickly becomes entangled in a web of hopeless integrals. While these may be computed numerically for finite loop graphs, many of the more complicated divergent loop integrals remain elusive. Thus, one would like to find a new method for evaluating graphs which avoids the shortcomings of these techniques and also allows for consistent regularization and renormalization schemes. Furthermore, it would be beneficial to maintain the desirable KSW power counting. Other subtraction schemes [7,8] have recently been developed that obey the KSW scaling, but none of these simplify the calculation of higher order contributions.

In this spirit, a consistent regularization and subtraction scheme is developed for non-relativistic field theories. In particular, the KSW effective field theory is used throughout to develop the methods. The same recipe is applicable to all diagrams. Loop integrals are transformed to coordinate space and divergences are transformed into divergences in a parameter with units of energy, where they are consistently treated. The results are seen to be totally consistent with dimensional regularization and PDS (or $\overline{MS}$) in the known cases. In addition, the coordinate space-parameter subtraction method, which we choose to call CPS, is easily extended well beyond the realm of the standard techniques in calculating higher order loop graphs. In section II the general methods are developed for bound state graphs. We show how calculate 2-pion exchange bound state graphs with an incident photon in the zero momentum limit, which is necessary for the NNLO calculation of the deuteron quadrupole moment. In section III, the results are generalized to finite photon momentum transfer graphs and above threshold scattering graphs. These examples serve to illustrate how graphs of any order may be obtained in terms of analytic functions. Section IV reviews the KSW effective field theory and the calculation of electromagnetic properties. Section V details the calculation of the deuteron quadrupole moment and the results are shown.

II. BOUND STATE GRAPHS

In Ref.[5], the deuteron electromagnetic form factors are calculated to NLO. Calculation of the full form factors at NNLO requires several graphs, the most difficult of which is the 2 pion exchange with a finite momentum photon attached on one side (Fig.1). First, we show how to evaluate the

FIGURES

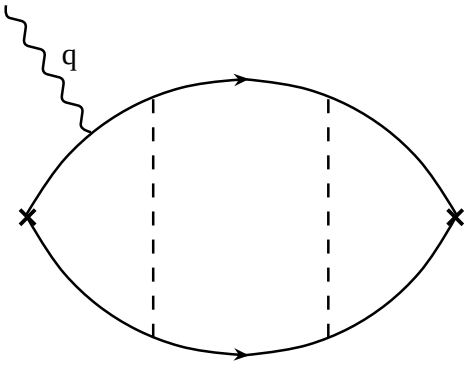

Fig.1 *Two potential pion exchange graph that gives a contribution to the deuteron quadrupole moment at NNLO. The photon corresponds to* A^0.

graph at zero momentum transfer. This will serve to introduce the CPS method, since this complicated graph contains almost all possible classes of loop integrals that might occur in bound state problems.

In the EFT of Kaplan, Savage, and Wise we find an amplitude for Fig.1 of

$$\mathcal{A} = \frac{-9g^4 M_N^4 e}{2f^4} \int \frac{d\tilde{p}d\tilde{l}d\tilde{k}(2l_i k_j l\cdot k - l_i l_j k^2 - k_i k_j l^2 + \frac{1}{2}l^2 k^2 \delta_{ij})}{((p-q/2)^2+\gamma^2)(p^2+a^2)((p+l)^2+a^2)((p+l+k)^2+a^2)(l^2+m_\pi^2)(k^2+m_\pi^2)} \tag{1}$$

where $d\tilde{p} = \frac{d^3p}{(2\pi)^3}$, q is the photon 3-momenta, $p = \vec{p}$, $l = \vec{l}$, $k = \vec{k}$, $\gamma = \sqrt{-EM_N}$, $m_\pi = 138$MeV is the pion mass, $a = \sqrt{\gamma^2 + \frac{q^2}{4}}$, and i,j are the initial and final deuteron spin indices, respectively. We wish to extract the quadrupole moment part at zero momentum transfer. After straightforward but tedious convolutions and projections, the numerator of eq.(1) can be written in terms of p^2, l^2, k^2, $(p-l)^2$, and $(p+k)^2$ as 54 independent terms such as $(p-l)^4(p+k)^2 l^2 k^2/p^4$, $k^2 l^4$, and other products of squares of the momentum variables. Note the appearance of $1/p^4$ terms; these will introduce artificial infrared divergences which must cancel in the end. After all these steps, one is left with integrals over products of 1, 3, 4, and 5 propagators. Note that the $(p-l)^2$ propagator is raised to the fourth power from the Taylor expansion.

Let $I(n)$, $J(n)$, $K(n)$, and $L(n)$ be 1, 3, 4, and 5 propagator integrals with the $(p-l)^2$ propagator raised to the nth power. We now explicitly show how to calculate these integrals in CPS.

1-PROPAGATOR INTEGRALS

By definition $I_\gamma(n) \equiv \int d\tilde{p} \frac{1}{(p^2+\gamma^2)^n}$. Transforming to coordinate space we have

$$I_\gamma(1) = \int d\tilde{p} \int d^3x G_\gamma(x) e^{-i\vec{p}\cdot\vec{x}}, \tag{2}$$

where $G_\gamma(x) = \frac{e^{-\gamma x}}{4\pi x}$ is the Fourier transform of the propagator. Trivially $I_\gamma(1) = G_\gamma(0) = \frac{1}{4\pi}(1/x - \gamma)|_{x=0}$. Labelling the divergence μ we have

$$I_\gamma(1) = \frac{\mu - \gamma}{4\pi}. \tag{3}$$

Alternatively we could have differentiated with respect to γ and integrated back, yielding $I_\gamma(1) = -\int_\infty^\gamma d\gamma 2\gamma \int d^3x (G_\gamma(x))^2$, which becomes $I_\gamma(1) = -\int_\infty^\gamma d\gamma \frac{1}{4\pi} = \frac{\gamma|_\infty - \gamma}{4\pi}$. Labelling the linear parameter divergence as μ we have eq.(3). In fact, eq.(3) is exactly what would be obtained using dimensional regularization and PDS. This is a general result : poles in 3 dimensions using dimensional regularization and PDS are linear parameter divergences in CPS. Other $I_\gamma(n)$ for $n > 1$ are obtained easily by differentiating eq.(3) with respect to γ. We also have integrals of the form $IO \equiv \int d\tilde{p} \frac{1}{p^2}$, for which we let $\gamma \to 0$ in the above. Hence,

$$IO = \frac{\mu}{4\pi}. \tag{4}$$

The standard DR dictum that scaleless integrals are zero seems to indicate that CPS is not equivalent to dimensional regularization and PDS in eq.(4). However, scaleless integrals should only be zero when 4 dimensional logarithmic divergences are considered, such as in $\overline{MS}$, since then there is only one scale (the renormalization scale) with which to make a dimensionless argument for the logarithm. But for power law divergences, as in PDS, all we need is one scale, the renormalization scale. Thus, the natural extension of dimensional regularization to PDS is equivalent to eq.(4). Finally, we consider $IZ \equiv \int d\tilde{p} \frac{1}{p^4}$. After Fourier transforming and performing the integrals, we are left with $IZ = \frac{1}{4\pi} \int_0^\infty dx$. Labelling the linear coordinate divergence as ν we have

$$IZ = \frac{\nu}{4\pi}. \tag{5}$$

The same result is obtained by letting $\gamma \to 0$ in $I(2) = \frac{1}{8\pi\gamma}$ and then $\frac{1}{\gamma}|_{\gamma=0} \to 2\nu$. For our purposes it is not really important how one labels these artificial infrared divergences since a conspiracy amongst the 54 terms must cancel them in the end.

3-PROPAGATOR INTEGRALS

By definition

$$J(n) \equiv \int d\tilde{p} d\tilde{l} \frac{1}{(p^2 + \gamma^2)((p-l)^2 + \gamma^2)^n (l^2 + m_\pi^2)}. \tag{6}$$

In coordinate space we have

$$J(1) = \int d\tilde{p} d\tilde{l} d^3x d^3y d^3z G_\gamma(x) G_\gamma(y) G_{m_\pi}(z) e^{-i[\vec{p}\cdot\vec{x} + (\vec{p} - \vec{l})\cdot\vec{y} + \vec{l}\cdot\vec{z}]}. \tag{7}$$

This quickly reduces to $J(1) = \int d^3x d^3y d^3z G_\gamma(x) G_\gamma(y) G_{m_\pi}(z) \delta(\vec{x} + \vec{y}) \delta(\vec{y} - \vec{z}) = \frac{1}{16\pi^2} \int_0^\infty dx \frac{e^{-bx}}{x}$, where $b = 2\gamma + m_\pi$. Differentiating with respect to b, we have $J(1) = \frac{-1}{16\pi^2} \int_\infty^b db \frac{1}{b} = \frac{-1}{16\pi^2} [\log b - \log b|_\infty]$. Hence,

$$J(1) = \frac{-1}{16\pi^2} \log \frac{2\gamma + m_\pi}{\mu}. \tag{8}$$

Again, this is the same result obtained using DR and PDS or $\overline{MS}$, but those require substantially more effort. In general, four dimensional logarithmic divergences of dimensional regularization become logarithmic parameter divergences in CPS. Using the same methods we can derive

$$\begin{aligned} JO(1) &\equiv \int d\tilde{p} d\tilde{l} \frac{1}{p^2((p-l)^2 + \gamma^2)(l^2 + m_\pi^2)} \\ &= \frac{-1}{16\pi^2} \log \frac{\gamma + m_\pi}{\mu}. \end{aligned} \tag{9}$$

and

$$\begin{aligned} JZ(1) &\equiv \int d\tilde{p} d\tilde{l} \frac{1}{p^4((p-l)^2 + \gamma^2)(l^2 + m_\pi^2)} \\ &= \frac{2\nu(m_\pi + \gamma) - 1}{32\pi^2(\gamma + m_\pi)^2}, \end{aligned} \tag{10}$$

where ν is defined after eq.(5). Of course we get $J(n)$, $JO(n)$, and $JZ(n)$ for $n > 1$ by differentiation with respect to γ.

4-PROPAGATOR INTEGRALS

There are several different classes of 4-propagator integrals. The first is

$$K(n) \equiv \int d\tilde{p} d\tilde{l} d\tilde{k} \frac{1}{((p-l)^2 + \gamma^2)^n ((p+k)^2 + \gamma^2)(l^2 + m_\pi^2)(k^2 + m_\pi^2)}, \tag{11}$$

which contains both 3 and 4 dimensional poles in dimensional regularization. In configuration space we obtain $K(1) = \int d^3x (G_\gamma(x))^2 (G_{m_\pi}(x))^2 = \frac{1}{64\pi^3} \int_0^\infty dx \frac{e^{-\alpha x}}{x^2}$, where $\alpha = 2(m_\pi + \gamma)$. By partial integration $K(1) = \frac{1}{64\pi^3} [-\frac{e^{-\alpha x}}{x}|_0^\infty - \alpha \int_0^\infty dx \frac{e^{-\alpha x}}{x}]$. Hence the divergences are manifested as the linear and logarithmic poles seen before in eq.(3) and eq.(8). The result is

$$K(1) = \frac{1}{64\pi^3} [2(m_\pi + \gamma)(\log \frac{2(m_\pi + \gamma)}{\mu} - 1) + \mu]. \tag{12}$$

Next we consider integrals of the form

$$KP(n) \equiv \int d\tilde{p} d\tilde{l} d\tilde{k} \frac{p^2}{((p-l)^2 + \gamma^2)^n ((p+k)^2 + \gamma^2)(l^2 + m_\pi^2)(k^2 + m_\pi^2)}. \tag{13}$$

This is greatly complicated by the appearance of p^2 in the numerator which cannot be decoupled with momenta in the denominator. But one can evaluate the integral simply by using $p^2 = \int d^3x \delta(\vec{x})(-\nabla_x^2) e^{-i\vec{p}\cdot\vec{x}}$. It follows that

$$KP(1) = -\int d^3x d^3y d^3z G_\gamma(y) G_\gamma(z) G_{m_\pi}(y) G_{m_\pi}(z) \delta(\vec{x}) \nabla_x^2 \delta(\vec{x} + \vec{y} + \vec{z}) \tag{14}$$

where the derivative operator acts only on the delta function. Now we use $\int d^3x f(\vec{x})\nabla_x^2\delta(\vec{x}) = f''|_{x=0}$, where the primes denote operation by ∇_x^2. Thus,

$$\begin{aligned} KP(1) &= -\int d^3y d^3z G_\gamma(y)G_\gamma(z)G_{m_\pi}(y)G_{m_\pi}(z)\delta''(\vec{y}+\vec{z}) \\ &= -\int d^3y G_\gamma(y)G_{m_\pi}(y)[G_\gamma(y)G_{m_\pi}(y)]'' \end{aligned} \tag{15}$$

From the definition of $G_\gamma(x)$ we find

$$\begin{aligned} \vec{\nabla}_x\, G_\gamma(x) &= 0 \\ \nabla_x^2 G_\gamma(x) &= \gamma^2 G_\gamma(x) - \delta(\vec{x}). \end{aligned} \tag{16}$$

Straightforwardly,

$$\begin{aligned} KP(1) &= G_\gamma(y)(G_{m_\pi}(y))^2|_{y=0} + (G_\gamma(y))^2 G_{m_\pi}(y)|_{y=0} - (\gamma^2+m_\pi^2)\int d^3y (G_\gamma(y))^2(G_{m_\pi}(y))^2 \\ &= I_\gamma^2(1)I_{m_\pi}(1) + I_\gamma(1)I_{m_\pi}^2(1) - (\gamma^2+m_\pi^2)K(1). \end{aligned} \tag{17}$$

We must also deal with $KPP(n)$, which is the same as $KP(n)$ except the numerator is p^4 instead of p^2. This is obtained in similar fashion and the only new result needed is $\nabla_x^4 G_\gamma(x) = \gamma^4 G_\gamma(x) - \gamma^2\delta(\vec{x}) - \delta''(\vec{x})$. We obtain

$$KPP(1) = (\gamma^2+m_\pi^2)^2K(1) - 2(2\gamma^2+m_\pi^2)I_\gamma^2(1)I_{m_\pi}(1) - 2(\gamma^2+2m_\pi^2)I_\gamma(1)I_{m_\pi}^2(1). \tag{18}$$

5-PROPAGATOR INTEGRALS

Finally, we come to the master integrals for 2 pion exchange graphs. By definition

$$L(n) \equiv \int d\tilde{p}d\tilde{l}d\tilde{k}\frac{1}{(p^2+a^2)((p-l)^2+\gamma^2)^n((p+k)^2+\gamma^2)(l^2+m_\pi^2)(k^2+m_\pi^2)}, \tag{19}$$

where a will be set to γ in the end, but we label it differently for reasons that will be clear. After the delta function integrations in coordinate space we arrive at

$$\begin{aligned} L(1) &= \frac{1}{(4\pi)^5}\int d^3x d^3y \frac{e^{-(\gamma+m_\pi)(x+y)-a|\vec{x}-\vec{y}|}}{x^2y^2|\,\vec{x}-\vec{y}\,|} \\ &= \frac{1}{2a(4\pi)^3}\int_0^\infty dx\int_0^\infty dy\frac{e^{-(\gamma+m_\pi)(x+y)}}{xy}[e^{-a|x-y|}-e^{-a(x+y)}] \\ &\equiv \frac{1}{2a(4\pi)^3}I_L, \end{aligned} \tag{20}$$

where we have performed the angular integrations in the last step and defined I_L in the obvious manner. Now use the symmetry between x and y to write

$$\begin{aligned} I_L &= 2\int_0^\infty \frac{dx}{x}\int_0^x \frac{dy}{y}e^{-(\gamma+m)(x+y)}[e^{-a(x-y)}-e^{-a(x+y)}] \\ &\equiv I_L^A - I_L^B. \end{aligned} \tag{21}$$

One must be careful here. We used the property that the integrand is symmetric in $x \leftrightarrow y$ to get rid of the troublesome absolute value. But this must be done for both pieces, since $L(1)$ is finite but each individual piece I_L^A and I_L^B is divergent. The wrong answer would be obtained by exploiting the symmetry in I_L^A, but not I_L^B. This is a consequence of the following simple rule : only finite integrals may be exploited for their symmetry properties as above, since otherwise information is lost about the relationship between the artificial divergences. In splitting a finite integral into several divergent pieces, every piece must be dealt with in the same manner. Now $I_L^A = 2\int_0^\infty \frac{dx}{x}\int_0^x \frac{dy}{y} e^{-bx-\tilde{m}y}$, where $b = m_\pi + \gamma + a$ and $\tilde{m} = m_\pi + \gamma - a$. We only need evaluate I_L^A explicitly since $I_L^B = I_L^A(\tilde{m} \rightarrow b)$. Differentiating with respect to b and $\tilde{m}$ we have

$$\begin{aligned} I_L^A &= -2\int_\infty^{\tilde{m}} d\tilde{m} \int_0^\infty \frac{dx}{x}\int_0^x dy e^{-bx-\tilde{m}y} \\ &= -2\int_\infty^{\tilde{m}} \frac{d\tilde{m}}{\tilde{m}} \int_\infty^b db \int_0^\infty dx e^{-bx}(e^{-\tilde{m}x} - 1) \\ &= -2\int_\infty^{\tilde{m}} \frac{d\tilde{m}}{\tilde{m}} \int_\infty^b db (\frac{1}{\tilde{m}+b} - \frac{1}{b}) \\ &= -2\int_\infty^{\tilde{m}} \frac{d\tilde{m}}{\tilde{m}} (\log\frac{\tilde{m}+b}{\mu} - \log\frac{b}{\mu}), \end{aligned} \tag{22}$$

where we have used the CPS prescription for the artificial logarithmic divergences. Next we employ

$$\int dx \frac{\log(x+y)}{x} = \log x \log y - \mathrm{Polylog}_2(-\frac{x}{y}), \tag{23}$$

whence we deduce

$$I_L^A = 2\mathrm{Polylog}_2(-\frac{\tilde{m}}{b})\Big|_\infty^{\tilde{m}}. \tag{24}$$

The polylogarithms are generalized logarithms and may be defined by $\mathrm{Polylog}_n(x) = \sum_{i=1}^\infty \frac{x^i}{i^n}$. It can easily be shown that for large x, $\mathrm{Polylog}_2(-x) \rightarrow -\frac{(\log x)^2}{2} - \frac{\pi^2}{6}$. Thus,

$$I_L^A = 2[\mathrm{Polylog}_2(\frac{-\tilde{m}}{b}) + \frac{(\log\frac{b}{\mu})^2}{2} + \frac{\pi^2}{6}] \tag{25}$$

and from this we obtain $I_L^B = 2[\frac{(\log\frac{b}{\mu})^2}{2} + \frac{\pi^2}{12}]$, so that $I_L = 2[\mathrm{Polylog}_2(\frac{-\tilde{m}}{b}) + \frac{\pi^2}{12}]$. Hence, we finally have

$$\begin{aligned} L(1) &= \frac{1}{(4\pi)^3 a}[\mathrm{Polylog}_2(\frac{a - m_\pi - \gamma}{a + m_\pi + \gamma}) + \frac{\pi^2}{12}] \\ &= \frac{1}{(4\pi)^3 \gamma}[\mathrm{Polylog}_2(\frac{-m_\pi}{m_\pi + 2\gamma}) + \frac{\pi^2}{12}] \end{aligned} \tag{26}$$

$L(2)$ may be obtained by differentiating this with respect to γ. One might hope to get $L(n)$ for $n > 2$ similarly, but because the $x \leftrightarrow y$ symmetry was

required, we can not label the 2 γ's in eq.(19) differently and then differentiate. However, we can obtain $L(3)$ and $L(4)$ by differentiating eq.(26) with respect to γ and using the following integral which is easily calculated :

$$L22 \equiv \int d\tilde{p}d\tilde{l}d\tilde{k}\frac{1}{(p^2+a^2)((p-l)^2+\gamma^2)^2((p+k)^2+\gamma^2)^2(l^2+m_\pi^2)(k^2+m_\pi^2)}$$
$$= \frac{1}{8\gamma^2(4\pi)^3(m_\pi+a+\gamma)^2(m_\pi+\gamma)}. \tag{27}$$

By explicit calculation or by taking $a\rightarrow 0$ in eq.(26) we arrive at

$$LO(1) \equiv \int d\tilde{p}d\tilde{l}d\tilde{k}\frac{1}{p^2((p-l)^2+\gamma^2)((p+k)^2+\gamma^2)(l^2+m_\pi^2)(k^2+m_\pi^2)}$$
$$= \frac{2\log 2}{(4\pi)^3(m_\pi+\gamma)}. \tag{28}$$

Similarly, recall $\frac{1}{a}|_{a=0}\rightarrow 2\nu$, and find

$$LZ(1) \equiv \int d\tilde{p}d\tilde{l}d\tilde{k}\frac{1}{p^4((p-l)^2+\gamma^2)((p+k)^2+\gamma^2)(l^2+m_\pi^2)(k^2+m_\pi^2)}$$
$$= \frac{1}{(4\pi)^3(m_\pi+\gamma)^3}[\nu(m_\pi+\gamma)-\frac{2\log 2+1}{3}]. \tag{29}$$

$LO(n)$ and $LZ(n)$ for $n>1$ are obtained similarly. Note that $L(n)$ and $LO(n)$ are finite and $LZ(n)$ contains artificial infrared divergences, as expected.

This exhausts our treatment of the integrals necessary to calculate Fig.1. A few comments are in order. In the CPS system the regularization and subtraction are done in the same step. The scale μ can be viewed as a label for the divergence and also as the renormalization scale. The counterterms introduced to subtract the infinities satisfy the local symmetries of the Lagrange density. Specifically, gauge invariance and Euclidean invariance are easily seen to be preserved by the CPS regulator because the poles in CPS are isomorphic with poles in dimensional regularization, at least to the order we are working. This equivalence also implies that the KSW power counting scaling is preserved and the CPS scheme may be consistently implemented with other PDS calculations. Particularly, in section V the previously determined numerical values for the NLO counterterm coefficients C_2 and D_2 [1] are used with CPS calculated amplitudes for the deuteron quadrupole moment. Also note that the derivation of these integrals does not change as we go above threshhold, so analogous results can be obtained with the prescription $\gamma\rightarrow -ip$. The application of these methods to higher order diagrams, such as the 3 potential pion exchange graph analogous to Fig.1, is straightforward. For example, the master integral for the 3 pion exchange graph, involving seven propagators, is expressed in terms of Polylog of order 3 and lower. In general, an n-pion exchange graph can be expressed in terms of Polylog_n and lower order polylogarithms.

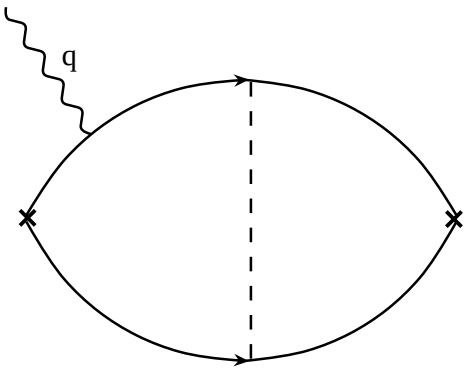

Fig.2.*Photon coupled to a deuteron bound state with one pion exchange. This gives the deuteron quadrupole moment at NLO.*

III. FINITE MOMENTUM TRANSFER GRAPHS AND ABOVE THRESHHOLD SCATTERING

Now it is shown how to calculate bound state graphs with finite momentum transfer. For pedagogical reasons we begin with a simpler graph than Fig.1. The analogous one pion exchange graph shown in Fig.2 serves to illustrate CPS extension to the $q{\neq}0$ case.

Again, in the effective field theory of [1], we find a Born amplitude of

$$\mathcal{A} = \frac{-3eg^2M_N^3}{2f^2}\int d\tilde{p}d\tilde{l}\frac{2l_il_j - l^2\delta_{ij}}{((p-q/2)^2+\gamma^2)(p^2+a^2)((p+l)^2+a^2)(l^2+m_\pi^2)}. \tag{30}$$

To extract the contribution to the electric quadrupole or monopole form factor, we multiply by the appropriate orthogonal tensor structure. These are $Q_{ij} = q_iq_j - \frac{q^2\delta_{ij}}{3}$ and δ_{ij}, respectively. Depending on which structure is desired, different integrals will be needed. But in both cases the master integral is

$$\begin{aligned} I &\equiv \int d\tilde{p}d\tilde{l}\frac{1}{((p-q/2)^2+\gamma^2)(p^2+a^2)((p+l)^2+a^2)(l^2+m_\pi^2)} \\ &= \frac{1}{(4\pi)^4}\int d^3xd^3y\frac{\exp\left[-(a+m_\pi)x - ay - \gamma|\ \vec{x}-\vec{y}\ | + i\frac{\vec{q}\cdot(\vec{x}-\vec{y})}{2}\right]}{x^2y|\ \vec{x}-\vec{y}\ |} \end{aligned} \tag{31}$$

where the trivial delta function integrations have been performed after going to coordinate space. Now we write $\vec{q}\cdot(\vec{x}-\vec{y}){\equiv}q|\vec{x}-\vec{y}|u_q$ and $\tilde{\gamma} = \gamma - \frac{iqu_q}{2}$, where $u_q = \cos\theta_q$ will be averaged over later. In familiar fashion, the angular integrations are performed and a sum of 2 artificially divergent integrals remains :

$$I = \frac{1}{32\pi^2\tilde{\gamma}}\int_0^\infty\frac{dx}{x}\int_0^\infty dye^{-(a+m_\pi)x-ay}(e^{-\tilde{\gamma}|x-y|} - e^{-\tilde{\gamma}(x+y)}). \tag{32}$$

Using the methods developed above, and being sure to treat the two terms in an equivalent manner, the following result is quickly obtained :

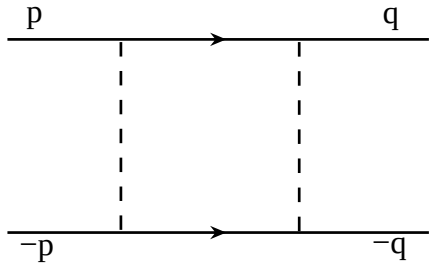

Fig.3.*Box diagram contributing to the NNLO scattering amplitude.*

$$I = \frac{1}{32\pi^2\tilde{\gamma}}(\frac{1}{\tilde{\gamma}-a}+\frac{1}{\tilde{\gamma}+a})\log\frac{m_\pi+a+\tilde{\gamma}}{m_\pi+2a}. \tag{33}$$

Now we must perform the u_q integration. Using eq.(23) and after some algebra the integral becomes

$$I = \frac{1}{32\pi^2 aq}\{2\Im[\mathrm{Polylog}_2(\frac{a-\gamma-iq/2}{m_\pi+2a})+\mathrm{Polylog}_2(\frac{-a-\gamma-iq/2}{m_\pi})]+\log\Big[1+\frac{2a}{m}\Big]\arctan\frac{q}{2\gamma}\} \tag{34}$$

Although this is more complicated than the zero momentum transfer integral, eq.(8), we still obtain a nice closed form solution. Similarly, we can derive an expression for the two pion exchange graph shown in Fig.1 at finite momentum transfer. The result is in terms $\mathrm{Polylog}_3$ and lower order polylogarithms and logarithms.

Now we briefly comment on above threshold scattering graphs such as the box diagram in Fig.3, where $\vec{p}$ and $\vec{q}$ are the initial and final state momenta, and i and j are the spin indices for the initial and final states, respectively. The same techniques can be used for $S\to S$, $S\to D$, and $D\to D$ wave scattering. In any case, the momenta in the numerator of the loop integral may be decoupled with the propagator momenta, so that only 1, 2, and 3 propagator integrals are left. The master integral is

$$I = \int d\tilde{l}\frac{1}{(l^2-p^2)((l-p)^2+m_\pi^2)((q-l)^2+m_\pi^2)}. \tag{35}$$

After the delta function integrations in coordinate space

$$I = \frac{1}{(4\pi)^3}\int d^3x d^3y \frac{\exp\left[ipy-m_\pi x-m_\pi|\vec{x}+\vec{y}|+i\,\vec{p}\cdot\vec{x}-i\,\vec{q}\cdot(\vec{x}+\vec{y})\right]}{xy|\vec{x}+\vec{y}|} \tag{36}$$

Averaging over the angles of p we have

$$I = \frac{1}{(4\pi)^3 ip}\int d^3x d^3y \frac{\exp\left[ipy-m_\pi x-m_\pi|\vec{x}+\vec{y}|-i\,\vec{q}\cdot(\vec{x}+\vec{y})\right]}{x^2y|\vec{x}+\vec{y}|}[e^{ipx}-e^{-ipx}]. \tag{37}$$

But this is exactly the same form of eq.(31), and we can proceed almost identically. The similarity in the derivation of these two loop integrals is no accident. Both for bound state graphs with finite momentum transferred into the loop, and for above threshhold scattering graphs, we have an external momentum flow into the internal loop structure.

IV. CALCULATING ELECTROMAGNETIC PROPERTIES IN EFFECTIVE NUCLEAR FIELD THEORY

Here we only briefly review the pertinent aspects of the KSW effective field theory and the tools necessary to calculate electromagetic properties. The Lagrange density with pions and nucleons is written as [1]

$$\mathcal{L} = \mathcal{L}_0 + \mathcal{L}_1 + \mathcal{L}_2 + ... \tag{38}$$

where $\mathcal{L}_n$ contains n-body nucleon operators. Here

$$\mathcal{L}_0 = \frac{1}{2}(\mathbf{E}^2 - \mathbf{B}^2) + \frac{f^2}{8}\mathrm{Tr}D_\mu \Sigma D^\mu \Sigma^\dagger + \frac{f^2}{4}\lambda \mathrm{Tr} m_q(\Sigma + \Sigma^\dagger) + ... \tag{39}$$

where $m_q = \mathrm{diag}(m_u, m_d)$, $m_\pi^2 = \lambda(m_u + m_d)$, $f = 132\mathrm{MeV}$ is the pion decay constant, and the covariant derivative acting on Σ is

$$D_\mu \Sigma = \partial_\mu \Sigma + ie[Q_{em}, \Sigma]A_\mu. \tag{40}$$

The one-body terms are

$$\mathcal{L}_1 = N^\dagger(iD_0 + \frac{\mathbf{D}^2}{2M})N + \frac{ig_A}{2}N^\dagger \sigma \cdot (\xi \mathbf{D}\xi^\dagger - \xi^\dagger \mathbf{D}\xi)N + ... \tag{41}$$

where the covariant derivative acting on the nucleon fields is

$$D_\mu N = (\partial_\mu + ieQ_{em}A_\mu)N. \tag{42}$$

The two-body operators relevant to the present work is

$$\begin{aligned}\mathcal{L}_2 = &-(C_0 + D_2\lambda \mathrm{Tr} m_q)(N^T P_i N)^\dagger (N^T P_i N) + \frac{C_2}{8}[(N^T P_i N)^\dagger (N^T P_i \overleftrightarrow{D}^2 N) + h.c.] \\ &+ \frac{C_2^{S\to D}}{8}\{(N^T P_i N)^\dagger (N^T P_\alpha [\overleftrightarrow{D}_\alpha \overleftrightarrow{D}_i - \overleftrightarrow{D}^2 \frac{\delta_{i\alpha}}{3}]N) + h.c.\} + ...\end{aligned} \tag{43}$$

where $P_i \equiv \frac{1}{\sqrt{8}}\sigma_2\sigma_i\tau_2$ projects onto spin and isospin states in the spin triplet channel. Also, all of the above operators are assumed to be operators in the spin triplet channel, which is relevant to the deuteron. Three of the counterterms have been determined previously [1] to be

$$C_0 = -5.51\mathrm{fm}^2, C_2 = 9.91\mathrm{fm}^4, D_2 = 1.32\mathrm{fm}^4 \tag{44}$$

at renormalization scale $\mu = m_\pi$. Note in eq.(43) the presence of a new local four nucleon operator which mixes ${}^3S_1$ and ${}^3D_1$ wave states. This does not appear until NNLO because it scales like $1/Q$ in the power counting, unlike the other two derivative coupling, C_2, which scales as $1/Q^2$. The reason is that the C_2 operator can be renormalized by C_0 bubble chains on both sides whereas the $C_2^{S\to D}$ operator is only renormalized on the S wave side. The value of this counterterm will be determined in this paper. We also note that a direct quadrupole moment operator where the photon couples to the four nucleon vertex does not appear until NNNLO, so we can safely neglect it.

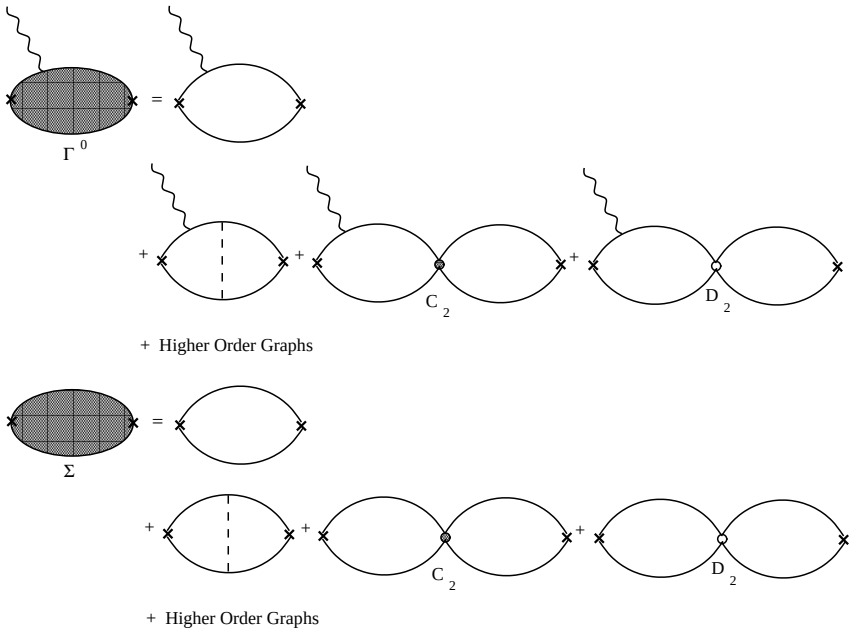

Fig.4. *A graphical expansion of the irreducible three-point functions (top) and the irreducible two-point functions (bottom). The first line in each case is the LO amplitude while the second lines are the NLO amplitudes. The dashed line represent potential pions, the 'X' marks are the deuteron interpolating fields which create or destroy a deuteron in the spin triplet channel.*

In ref.[5] the formalism necessary to calculate electromagnetic form factors in effective field theory were developed. The matrix element of the electromagnetic current is related to the irreducible 2-point and 3-point functions via

$$\langle \mathbf{p}\prime, j|J^{\mu}_{em}|\mathbf{p}, i\rangle = i\left[\frac{\Gamma^{\mu}_{ij}(\bar{E}\bar{E}', \mathbf{q})}{d\Sigma(\bar{E})/dE}\right]_{\bar{E},\bar{E}'\to -B}, \tag{45}$$

where Γ^{μ}_{ij} is the irreducible 3-point function, which is defined as the sum of all diagrams with two nucleons interacting with an external photon and each other such that the graph cannot be taken apart by cutting at a C_0 vertex. The irreducible 2-point function Σ is defined similarly, except in this case there are only two nucleons interacting with each other. The derivative of this 2-point function in eq.(45) is the wavefunction renormalization that arises from introducing the deuteron interpolating field

$$\mathcal{D}_i = N^T P_i N, \tag{46}$$

which annihilates a deuteron in a definite spin and isospin state. Also note that in eq.(45) $\mathbf{q} = \mathbf{p}' - \mathbf{p}$ is the photon momenta and $\bar{E}$ and $\bar{E}'$ are the center of mass energies.

The graphical expansions of the 2-point and 3-point functions up to NLO are shown in Fig.(4). The zeroth component of eq.(45) is related to the definitions of the form factors by

$$\langle \mathbf{p}\prime, j|J^0_{em}|\mathbf{p}, i\rangle = e[F_C(q^2)\delta_{ij} + \frac{1}{2M_d^2}F_Q(q^2)(\mathbf{q}_i\mathbf{q}_j - \frac{1}{3}q^2\delta_{ij})]. \tag{47}$$

For the present purposes, we need not consider the spatial components of this matrix element, since the quadrupole form factor $F_Q(q^2)$ is related to the quadrupole moment by

$$\frac{F_Q(0)}{M_d^2} = \mu_Q. \tag{48}$$

V. THE NNLO CALCULATION OF THE DEUTERON QUADRUPOLE MOMENT

The deuteron quadrupole moment was calculated in ref.[5] to NLO. The leading order contribution vanishes and the NLO result is given by

$$\mu_Q^{NLO} = \frac{g_A^2 M(6\gamma^2 + 9\gamma m_\pi + 4m_\pi^2)}{30\pi f^2(m_\pi + 2\gamma)^3}. \tag{49}$$

The numerical value for this is about 0.418fm^2, which is more than %40 larger than the experimental value of 0.2859fm^2. This is in very rough accordance with the expectation [1] that each order in the perturbative expansion is suppressed by about %30. A number of recent calculations [1–6] suggest that the expansion does in fact converge as expected in calculations up to NLO. However, there has not yet been a test of the theory at NNLO. Thus, it would be interesting to calculate the deuteron quadrupole moment at NNLO. Since it is only the second non-vanishing order, the errors are expected to be within %10, which is rivaling the accuracy of the most recent potential model calculations [9]. Calculations using potential models are consistently lower than the experimental value of the quadrupole moment by $\sim$%7. This suggests that dynamical considerations beyond potential interactions are needed to accutrately describe such systems. The effective field theory approach provides the systematic framework to account for these effects.

However, as mentioned previously, there is a new direct $S\to D$ wave operator at NNLO whose value is unfixed. One may expect to extract this value from low energy N-N scattering data in the spin triplet channel. The diagrams which give rise to this $\Delta L = 2$ $S\to D$ transition are shown in Fig.(5). Fitting these to the triplet channel mixing parameter ϵ_1 would yield the desired value of $C_2^{S\to D}$. However, new complications arise in the NNLO above threshhold scattering channel that are not present at lower orders nor in NNLO bound state problems. Work in this area is ongoing and will be presented later.

Alternatively, we can calculate the graphs necessary for the quadrupole moment and fit the new operator to the experimental value of μ_Q. This is the approach adopted in the present work. Thus, some of the questions raised in the preceding paragraph will have to wait until the NNLO triplet channel scattering analysis is complete. Several sources [10,11] suggest that perturbative potential pion exchange will give a large result compared

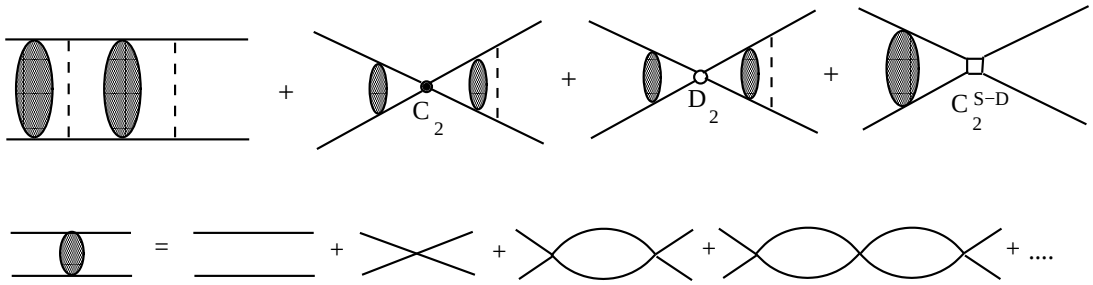

Fig.5. *The top line shows the graphs contributing to the* $^3S_1 \to {}^3D_1$ *wave scattering amplitude at NNLO. The bubble chain of* C_0 *operators is defined on the second line.*

with the counterterms. This expectation can be verified by the results presented here.

Expanding eq.(45) in powers of Q, which is the power counting scale in the KSW power counting scheme, we arrive at

$$\langle \mathbf{p}\prime, j|J^0_{em}|\mathbf{p}, i\rangle = i\Big[\frac{\Gamma^0_{(0)}}{d\Sigma_{(1)}/d\bar{E}}\Big] + i\Big[\frac{\Gamma^0_{(1)}d\Sigma_{(1)}/d\bar{E} - \Gamma^0_{(0)}d\Sigma_{(2)}/d\bar{E}}{(d\Sigma_{(1)}/d\bar{E})^2}\Big] + ..., \tag{50}$$

where we consider only the graphs that give a quadrupole contribution and

$$\begin{aligned}\Gamma^0 &= \Gamma^0_{(0)} + \Gamma^0_{(1)} + ... \\ \Sigma &= \Sigma_{(1)} + \Sigma_{(2)} + ...\end{aligned} \tag{51}$$

The first term in eq.(50) is the NLO result previously calculated while the other two terms are NNLO corrections. A number of diagrams occur at NNLO in the effective field theory power counting. Here we are only concerned with those that give rise to a quadrupole structure $Q_{ij} = q_i q_j - \frac{\delta_{ij}}{3}q^2$, where $\vec{q}$ is the photon 3-momenta. These diagrams must have a virtual $S \to D$ and then $D \to S$ transition. The graphs contributing to $\Gamma^0_{(1)}$ are shown in Fig.(6). The radiation pion refers simply to the graph evaluated by taking the pion pole in the energy integration rather than the nucleon poles. While the radiation pion graph (VI) shown in Fig.(6) occurs at NNLO and has a quadrupole contribution, the quadrupole piece itself is at NNNLO and can be safely neglected here. Furthermore, graph II is found to have a vanishing quadrupole contribution, which can be understood as follows. Any $S \to D$ transition from the first pion followed by a $D \to S$ transition from the photon will be exactly canceled by the reverse process, namely a $S \to D$ transition from the photon and then a $D \to S$ transition via the second pion. In other words, the photon interacts symmetrically with the deuteron, whereas assymmetries in the electromagnetic interaction give rise to the quadrupole moment. The remaining four graphs give non-vanishing contributions.

The C_2 and D_2 graphs are directly related to the NLO one pion exchange graph in Fig.(2) by

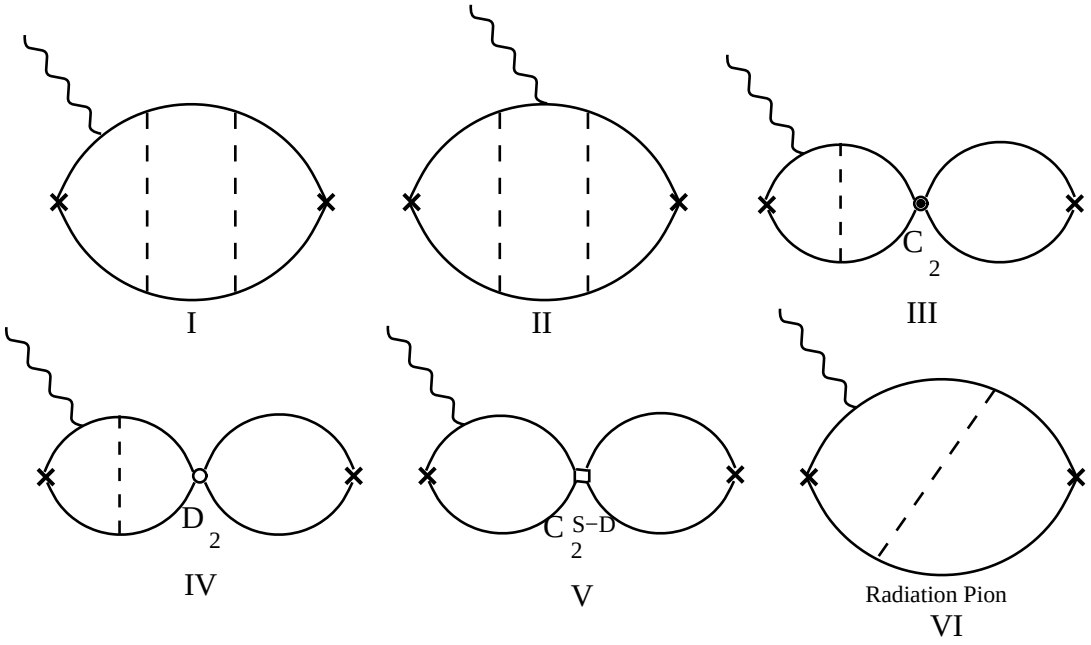

Fig.6. *The graphs contributing to the NNLO calculation of the deuteron quadrupole moment. The photon corresponds to* A^0.

$$\Gamma^0_{III} = \frac{\gamma^2 M_N C_2(\mu-\gamma)}{2\pi}\Gamma^0_{NLO}$$
$$\Gamma^0_{IV} = -\frac{m_\pi^2 M_N D_2(\mu-\gamma)}{2\pi}\Gamma^0_{NLO}. \tag{52}$$

The $C_2^{S\to D}$ graph (V) is given by

$$\Gamma^0_V = \frac{eM_N^3 C_2^{S\to D}(\mu-\gamma)}{384\gamma\pi^2}. \tag{53}$$

Finally, the two potential pion exchange graph is calculated using the CPS regularization and renormalization scheme developed in section II and determined to be

$$\begin{aligned}\Gamma^0_I = -\frac{9eg^4M_N^4}{5f^4}\Bigg\{&\Big[1280\gamma^9 + 3568\gamma^8 m_\pi + 4272\gamma^7 {m_\pi}^2 + 3296\gamma^6 {m_\pi}^3 + 1664\gamma^5 {m_\pi}^4 + 349\gamma^4 {m_\pi}^5 + 33\gamma^3 {m_\pi}^6 \\ &+ 60\gamma^2 {m_\pi}^7 + 18\gamma {m_\pi}^8 - 2\mu(520\gamma^8 + 1700\gamma^7 m_\pi + 2306\gamma^6 {m_\pi}^2 + 2007\gamma^5 {m_\pi}^3 + 1637\gamma^4 {m_\pi}^4 + 1215\gamma^3 {m_\pi}^5 \\ &+ 603\gamma^2 {m_\pi}^6 + 162\gamma {m_\pi}^7 + 18 {m_\pi}^8)\Big]/(294912\pi^3\gamma^5(\gamma+m_\pi)^2(2\gamma+m_\pi)^3) + \frac{\mu^2(\gamma^2+3{m_\pi}^2)}{24576\pi^3\gamma^5} \\ &- \frac{\mu\log\frac{\gamma+m_\pi}{2\gamma+m_\pi}}{3072\pi^3\gamma^2} + \frac{(7\gamma^2+{m_\pi}^2)\log\frac{2\gamma+m_\pi}{\mu}}{24576\pi^3\gamma^3} + \frac{{m_\pi}^2(3{m_\pi}^2-4\gamma^2)(\mathrm{Polylog}_2\Big[-\frac{m_\pi}{2\gamma+m_\pi}\Big]+\frac{\pi^2}{12})}{6144\pi^3\gamma^5} \\ &+ \frac{(180\gamma^5+340\gamma^4 m_\pi + 409\gamma^3 {m_\pi}^2 + 12\gamma^2 {m_\pi}^3 - 213\gamma {m_\pi}^4 - 72 {m_\pi}^5)\log\frac{2(\gamma+m_\pi)}{2\gamma+m_\pi}}{73728\pi^3\gamma^4(2\gamma+m_\pi)^2}\Bigg\}\end{aligned} \tag{54}$$

The expressions for the two-point functions are reproduced here and were calculated in [5] to be

$$\frac{d\Sigma_{(1)}}{d\bar{E}}\Big|_{\bar{E}=-B} = -i\frac{M_N^2}{8\pi\gamma}$$
$$\frac{d\Sigma_{(2)}}{d\bar{E}}\Big|_{\bar{E}=-B} = -i\frac{M_N^3}{16\pi^2\gamma}\Big[\frac{g_A^2}{2f^2}\Big(\gamma-\mu+\frac{m_\pi^2}{m_\pi+2\gamma}\Big)+D_2 m_\pi^2(\gamma-\mu)-C_2\gamma(\mu-\gamma)(\mu-2\gamma)\Big]. \quad (55)$$

The partial contributions to the quadrupole moment by graphs I, III, IV, and V are

$$\mu_Q^I = -16.7\text{fm}^2, \mu_Q^{III} = 0.079\text{fm}^2, \mu_Q^{IV} = -0.096\text{fm}^2, \quad (56)$$

and

$$\mu_Q^V = \frac{-(\mu-\gamma)C_2^{S\to D}M_N}{24\pi}. \quad (57)$$

Also, the last term of eq.(50) gives an additional wavefunction renormalization contribution of

$$\begin{aligned}\tilde{\mu}_Q &= -\frac{d\Sigma_{(2)}/d\bar{E}}{d\Sigma_{(1)}/d\bar{E}}\mu_Q^{NLO} \\ &= 0.203\text{fm}^2. \end{aligned} \quad (58)$$

The renormalization scale μ has been set to m_π but it should be noted that the running of the counterterms cancels the scale dependence to the order we are working. Fixing the counterterm $C_2^{S\to D}$ to reproduce the physical quadrupole moment yields a value of

$$C_2^{S\to D} = 5.1\text{fm}^4. \quad (59)$$

CONCLUSIONS

We have shown that otherwise comlicated loop diagrams arising in non-relativistic field theories, particularly the EFT of Kaplan, Savage, and Wise, can be easily calculated in a new regularization and renormalization scheme called CPS. The divergences are dealt with consistently by transforming them into divergences in a parameter with units of energy. This is done after the angular integrations in configuration space by inserting the identity operator in the form $\int_\infty^a da\frac{\partial}{\partial a}$, where a appears in the exponential. For artificial divergences such as the artificial infrared divergences arising in Fig.1, the only requirement is consistency in dealing with the infinities, since they cancel in the end. For real divergences, the CPS method precisely reproduces the results of dimensional regularization and PDS (or $\overline{MS}$) up to NLO. Higher order loop integrals evaluated in CPS also map onto poles in dimensional regularization. This gives one the power of the PDS subtraction scheme and the associated KSW power counting, without the calculational difficulties associated with dimensional regularization and Feynman parameters. As is the case with PDS, we could ignore the power law divergences and keep only the four dimensional logarithmic divergences, yielding a subtraction scheme similar to $\overline{MS}$. To illustrate the methods, the quadrupole moment of the deuteron is

calculated to three loops, thus fixing the numerical value of the direct four nucleon ${}^3S_1 \to {}^3D_1$ operator that appears at this order.

Although the emphasis in this paper has been effective field theories in nuclear physics, the techniques developed are applicable in other field theories, such as non-relativistic quantum chromodynamics (NRQCD).

ACKNOWLEDGEMENTS

This work was made possible by the generous hospitality and support of the Institute for Nuclear Theory during the past summer. The author would like to thank Eric Swanson, Martin Savage, and Jiunn-Wei Chen for useful discussions. Also, I thank Gautam Rupak, Noam Shoresh, and Harald Griesshammer for helpful comments and suggestions.

REFERENCES

[1] D.B. Kaplan, M.J. Savage, M.B. Wise, *Phys. Lett.* B **424** 390 (1998), nucl-th/9801034; nucl-th/9802075, *to appear in Nucl. Phys.* B.

[2] J.W. Chen, H.W. Griesshammer, M.J. Savage, R.P. Springer, nucl-th 9806080.

[3] M.J. Savage, R.P. Springer, nucl-th 9807014.

[4] D.B. Kaplan, M.J. Savage, R.P. Springer, M.B. Wise, nucl-th 9807081.

[5] D.B. Kaplan, M.J. Savage, M.B. Wise, nucl-th 9804032.

[6] M.J. Savage, K.A. Scaldeferri, M.B. Wise, nucl-th 9811029.

[7] T. Mehen and I.W. Stewart, nucl-th 9809071.

[8] T.D. Cohen and J.M. Hansen, nucl-th 9808006.

[9] B.S. Pudliner, V.R. Pandharipande, J. Carlson, S.C. Pieper, and R.B. Wiringa, nucl-th 9705009.

[10] T. Ericson and M. Rosa-Clot, *Ann. Rev. Nucl. Part. Sci.* **35** (1985) 271.

[11] D.Y. Wong, *Phys. Rev. Lett.* **2** (1959) 406.